Title

Therapeutic Cleavage of Anti–Aquaporin-4 Autoantibody in Neuromyelitis Optica by an IgG-Selective Proteinase

Journal

Molecular Pharmacology, 83(6)

ISSN

0026-895X

Authors

Tradtrantip, Lukmanee
Asavapanumas, Nithi
Verkman, AS

Publication Date

2013-06-01

DOI

10.1124/mol.113.086470

Peer reviewed

1521-0111/83/6/1268–1275$25.00
MOLECULAR PHARMACOLOGY

http://dx.doi.org/10.1124/mol.113.086470
Mol Pharmacol 83:1268–1275, June 2013

Therapeutic Cleavage of Anti–Aquaporin-4 Autoantibody in Neuromyelitis Optica by an IgG-Selective Proteinase

Lukmanee Tradtrantip, Nithi Asavapanumas, and A. S. Verkman

Departments of Medicine and Physiology, University of California, San Francisco, California

Received March 25, 2013; accepted April 9, 2013

ABSTRACT

Neuromyelitis optica (NMO) is an inflammatory demyelinating disease of the central nervous system caused by binding of pathogenic IgG autoantibodies (NMO-IgG) to astrocyte water channel aquaporin-4 (AQP4). Astrocyte damage and downstream inflammation require NMO-IgG effector function to initiate complement-dependent cytotoxicity (CDC) and antibody-dependent cell-mediated cytotoxicity (ADCC). Here, we evaluated the potential therapeutic utility of the bacterial enzyme IdeS (IgG-degrading enzyme of *Streptococcus pyogenes*), which selectively cleaves IgG antibodies to yield Fc and $F(ab')_2$ fragments. In AQP4-expressing cell cultures, IdeS treatment of monoclonal NMO-IgGs and NMO patient sera abolished CDC and ADCC, even when IdeS was added after NMO-IgG was bound to AQP4. Binding of NMO-IgG to AQP4 was similar to that of the NMO-$F(ab')_2$ generated by IdeS cleavage. NMO-$F(ab')_2$ competitively displaced pathogenic NMO-IgG, preventing cytotoxicity, and the Fc fragments generated by IdeS cleavage reduced CDC and ADCC. IdeS efficiently cleaved NMO-IgG in mice in vivo, and greatly reduced NMO lesions in mice administered NMO-IgG and human complement. IgG-selective cleavage by IdeS thus neutralizes NMO-IgG pathogenicity, and yields therapeutic $F(ab')_2$ and Fc fragments. IdeS treatment, by therapeutic apheresis or direct administration, may be beneficial in NMO.

Introduction

Neuromyelitis optica (NMO) is an autoimmune disease affecting the central nervous system, with inflammatory demyelinating lesions in the spinal cord and optic nerve and, to a lesser extent, in the brain (Wingerchuk et al., 2007; Jarius et al., 2008). A defining feature of NMO is the presence, in the majority of NMO patients, of serum IgG antibodies (NMO-IgG) directed against astrocyte water channel protein aquaporin-4 (AQP4) (Lennon et al., 2005; Jarius and Wildemann, 2010). AQP4 is concentrated in the foot processes of astrocytes throughout the central nervous system, as well as in supportive cells in neurosensory organs such as Müller cells in the retina, and in some peripheral organs including a subset of epithelial cells in the kidney, stomach, and the airways (Nielsen at al., 1997; Papadopoulos and Verkman, 2013). It is thought that NMO pathogenesis involves NMO-IgG binding to AQP4, which causes complement-dependent cytotoxicity (CDC) and antibody-dependent cell-mediated cytotoxicity (ADCC) (Lucchinetti et al., 2002; Kira, 2011; Papadopoulos and Verkman, 2012). The consequences of astrocyte damage include inflammation with cytokine release and infiltration of granulocytes and macrophages, disruption of the blood-brain barrier, and injury to oligodendrocytes and neurons. Current NMO therapies include immunosuppression, B cell depletion with anti-CD20 monoclonal antibody, and plasma exchange (Cree, 2008; Collongues and de Seze, 2011; Sato et al., 2012; Kim et al., 2013). New therapeutics are needed with improved efficacy and reduced long-term side effects.

NMO therapy targeting NMO-IgG binding to AQP4—the presumed initiating event in NMO pathogenesis—is attractive because of its potential specificity. We previously reported an engineered monoclonal, anti-AQP4 antibody lacking CDC and ADCC effector functions ("aquaporumab"; Tradtrantip et al., 2012b). Aquaporumab competes with pathogenic NMO-IgG for binding to AQP4, preventing downstream cytotoxicity and NMO pathology. As an alternative strategy, small-molecule blocking compounds were identified that reduce NMO-IgG binding to AQP4 (Tradtrantip et al., 2012a). Recently, we reported that deglycosylation of patient NMO-IgG by the IgG-selective enzyme endoglycosidase S (EndoS) neutralized its pathogenicity without affecting its binding to AQP4 (Tradtrantip et al., 2013). EndoS is a 108-kDa enzyme produced by *Streptococcus pyogenes* that digests asparagine-linked glycans on the heavy chain of all IgG subclasses (Collin and Olsen, 2001a).

Here, we investigated an alternative strategy to neutralize NMO-IgG pathogenicity using a proteinase from *S. pyogenes* that selectively cleaves IgG heavy chains in the hinge region to generate Fc and $F(ab')_2$ fragments (von Pawel-Rammingen et al., 2002; Vincents et al., 2004) (Fig. 1A). The enzyme, IdeS

This work was supported by grants from the Guthy-Jackson Charitable Foundation; and the National Institutes of Health [Grants DK35124, EY13574, EB00415, DK86125, and DK72517].
dx.doi.org/10.1124/mol.113.086470.

ABBREVIATIONS: ADCC, antibody-dependent cell-mediated cytotoxicity; AQP4, aquaporin-4; CDC, complement-dependent cytotoxicity; CHO, Chinese hamster ovary; EndoS, endoglycosidase S; GFAP, glial fibrillary acidic protein; IdeS, IgG-degrading enzyme of *Streptococcus pyogenes*; NK, natural killer; NMO, neuromyelitis optica; NMO-IgG, neuromyelitis optica immunoglobulin G; NMO-IgG^{IdeS}, IdeS-treated NMO-IgG; NMO $serum^{IdeS}$, IdeS-treated NMO serum; PBS, phosphate-buffered saline; PFA, paraformaldehyde; rAb, recombinant monoclonal antibody.

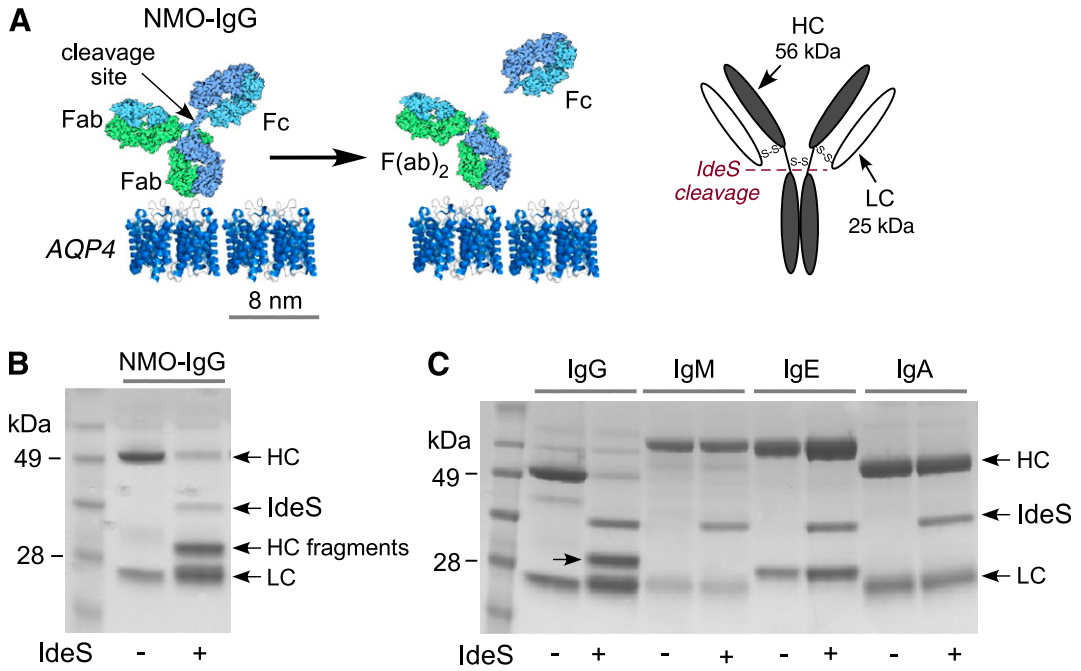

Fig. 1. IdeS cleavage of human NMO-IgG. (A) Schematic showing F(ab′)$_2$ and Fc fragments produced by IdeS cleavage of IgG heavy chains at lower hinge region. (B) Coomassie Blue SDS-PAGE of control and IdeS-treated NMO-IgG (rAb-53, 5 μg, 60-minute incubation with 5 U of IdeS at 37°C). (C) Selective IgG cleavage by IdeS. Coomassie Blue SDS-PAGE of control and IdeS-treated antibodies (1 μg of purified human antibodies incubated with 5 U of IdeS for 30 minutes at 37°C). HC, heavy chain; LC, light chain.

(IgG-degrading enzyme of *S. pyogenes*), also called Mac1, efficiently cleaves human IgGs of all subclasses without effect on other antibody classes or proteins. Compared with EndoS, IdeS 1) has a greater rate of IgG cleavage compared with the rate of EndoS deglycosylation, 2) produces antibody fragments with zero residual effector function, and 3) generates free Fc fragments that block Fc receptors on phagocytes. IdeS has shown efficacy in rodent models of experimental arthritis caused by anticollagen antibodies (Nandakumar et al., 2007), idiopathic thrombocytopenic purpura caused by antiplatelet antibodies (Johansson et al., 2008), and glomerulonephritis caused by antiglomerular basement membrane antibodies (Yang et al., 2010). IdeS represents a logical candidate to evaluate and potentially repurpose for NMO therapy, as another proteolytic enzyme from *S. pyogenes*, streptokinase, has been used for more than a decade as an effective, safe anticoagulant.

Materials and Methods

Cell Culture and Antibodies. Chinese hamster ovary (CHO) cells stably expressing human M23-AQP4 (Phuan et al., 2012) were cultured at 37°C in 5% CO_2/95% air in F-12 Ham's Nutrient mix medium (Sigma-Aldrich, St. Louis, MO) supplemented with 10% fetal bovine serum, 200 μg/ml geneticin (selection marker) (Invitrogen, Grand Island, NY), 100 units/ml penicillin, and 100 μg/ml streptomycin. Recombinant monoclonal NMO antibodies rAb-53 and rAb-93 were generated from a clonally expanded plasma blast population from the cerebrospinal fluid of an NMO patient (Bennett et al., 2009; Crane et al., 2011). NMO serum was obtained from NMO-IgG seropositive individuals who met the revised diagnostic criteria for clinical disease (Wingerchuk et al., 2006). Non-NMO (seronegative) human serum was used as control. For some studies, IgG was purified from NMO or control serum using a protein A resin (GenScript, Piscataway, NY) and concentrated using Amicon Ultra Centrifugal Filter Units (Millipore, Billerica, MA). Purified human IgM and IgA were purchased from Calbiochem (San Diego, CA), IgE from Abcam (Cambridge, MA), and IgG from Thermo Scientific Pierce (Rockford, IL).

IdeS Treatment. IdeS (FabRICATOR) and IdeS microspin column (FragIT Microspin) were purchased from Bulldog Bio Inc. (Rochester, NY). NMO-IgG or NMO serum (or control IgG/serum) was treated by incubation with IdeS (1–5 units per 1 μg of IgG) for up to 1 hour at 37°C; NMO serum was digested with IdeS using a microspin column containing IdeS covalently coupled to agarose beads. Treated antibody is referred to as NMO-IgG^{IdeS}. Treated NMO serum is referred to as NMO serum^{IdeS}. IdeS treatment was assessed by 10% SDS-PAGE followed by staining with Coomassie Blue.

NMO-IgG Binding. Cells were grown on glass coverslips for 24 hours. After blocking with 1% bovine serum albumin in phosphate-buffered saline (PBS), cells were incubated with NMO-IgG or NMO serum (control or IdeS-treated) for 30 minutes at room temperature. Cells were washed with PBS and incubated with Cy3-conjugated AffiniPure goat antihuman IgG, F(ab′)$_2$ fragment-specific, secondary antibody (1:200; Jackson ImmunoResearch, West Grove, PA). For AQP4 immunostaining, cells were fixed in 4% paraformaldehyde (PFA) and permeabilized with 0.2% Triton-X (Sigma-Aldrich). Rabbit anti-AQP4 antibody (1:200; Santa Cruz Biotechnology, Dallas, TX) was added followed by Alexa Fluor-488 goat antirabbit IgG secondary antibody (1:200; Invitrogen) for quantitative ratio image analysis (Crane et al., 2011).

To test whether the F(ab′)$_2$ fragments produced by IdeS cleavage compete with NMO-IgG for binding to AQP4, CHO-M23 cells were plated in black 96-well plates with clear plastic bottoms (Corning-Costar, Tewksbury, MA) at a density of 25,000 cells per well for 24 hours. After blocking with 1% bovine serum albumin in PBS, cells were incubated with NMO-IgG and NMO-IgG^{IdeS} or control-IgG^{IdeS} for 30 minutes at room temperature. Cells were washed with PBS and incubated with horseradish peroxidase–conjugated goat antihuman IgG, Fc fragment-specific, secondary antibody (1:500; Invitrogen) for 30 minutes. After washing each well three times with PBS, 50 μl of Amplex red substrate (100 μM; Sigma-Aldrich) and 2 mM H_2O_2 was

added for measurement of horseradish peroxidase activity. Fluorescence was measured after 45 minutes (excitation 540 nm, emission 590 nm).

CDC and ADCC Assays. For assay of CDC, cells were incubated for 60 minutes at 37°C with NMO-IgG or NMO serum (control or IdeS-treated) with 2% human complement (Innovative Research, Novi, MI). In some experiments, NMO-IgG was added 30 minutes before IdeS addition, followed 60 minutes later by complement. Cytotoxicity was measured by the Alamar Blue assay (Invitrogen). For assay of ADCC, natural killer (NK)-92 cells expressing CD16 (Conkwest, San Diego, CA) were used as the effector cells. The AQP4-expressing CHO cells were incubated for 1 hour at 37°C with NMO-IgG and effector cells at an effector:target cell ratio of 4:1. To test the effect of Fc fragments generated by IdeS cleavage on CDC, AQP4-expressing CHO cells were incubated for 1 hour with human IgG Fc fragments (Calbiochem) together with NMO-IgG (3 μg/ml rAb-53) and 1% human complement. To test the effect on ADCC, human IgG Fc fragments (Calbiochem) were preincubated with NK cells for 30 minutes at 37°C, then added together with NMO-IgG (3 μg/ml rAb-53) to AQP4-expressing CHO cells and incubated for 1 hour.

In Vivo Mouse Models of NMO. Adult wild-type mice (30–35 g) were anesthetized with 2,2,2-tribromoethanol (125 mg/kg i.p.) and mounted in a stereotactic frame. Following a midline scalp incision, a burr hole of diameter 1 mm was made in the skull 2 mm to the right of the bregma. A 30-gauge needle attached to a 50-μl gas-tight glass syringe (Hamilton, Reno, NV) was inserted 3 mm deep to infuse 0.6 μg of NMO-IgG (control or IdeS-treated) and 3 μl of human complement in a total volume of 8 μl (at 2 μl/min) (Saadoun et al., 2010). In some experiments, purified IgG from NMO serum (12 μg) was injected together with an excess of IdeS-treated IgG purified from NMO or control serum (48 μg) and 3 μl of human complement in a total volume of 18 μl. In some experiments, mice were injected with 0.6 μg of NMO-IgG and 15 minutes later, at the same site, with 3 μl of human complement with or without 16.75 U of IdeS. After three days, mice were anesthetized and perfused through the left cardiac ventricle with 5 ml of PBS and then 20 ml of PBS containing 4% PFA. Brains were postfixed for 2 hours in 4% PFA. Paraffin sections 5 μm thick were immunostained at room temperature for 1 hour with rabbit anti-AQP4 (1:200; Santa Cruz Biotechnology, Santa Cruz, CA), mouse anti-glial fibrillary acidic protein (GFAP) (1:100; Millipore, Temecula, CA), and goat anti–myelin basic protein (1:200; Santa Cruz Biotechnology) followed by the appropriate fluorescent secondary antibody (1:200; Invitrogen). Tissue sections were photographed using

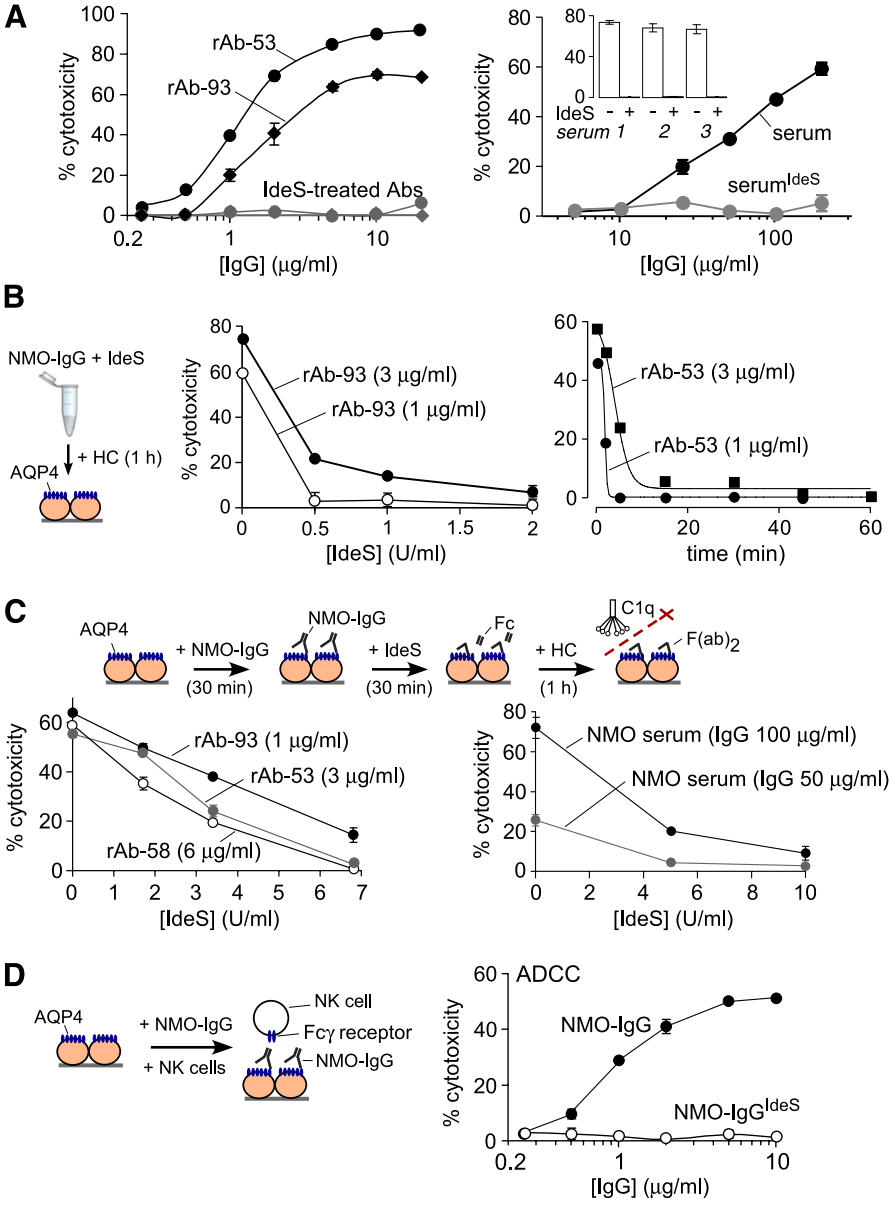

Fig. 2. IdeS treatment of NMO-IgG prevents CDC and ADCC. (A) CDC in AQP4-expressing CHO cells incubated for 60 minutes with control and IdeS-treated monoclonal recombinant NMO-IgGs (rAb-53, rAb-93; each 0.2–20 μg/ml) (left) and NMO sera (5–200 μg/ml) (right), each together with 2% human complement. Cytotoxicity quantified by Alamar Blue assay. (Inset) CDC for 3 different NMO sera (S.E., n = 4). (B) Time course and concentration dependence of IdeS action. (left) CDC was measured as in (A) for NMO-IgG rAb-93 (1 and 3 μg/ml), which was incubated for 30 minutes with indicated concentrations of IdeS prior to addition to cells. (Right) CDC measurement in which NMO-IgG rAb-53 (1 and 3 μg/ml) was incubated with 1.68 U/ml IdeS for indicated times prior to addition to cells (S.E., n = 4). (C) IdeS treatment of AQP4-bound NMO-IgG prevents CDC. Cells were incubated with NMO-IgGs or NMO serum for 30 minutes, then treated with IdeS for 30 minutes, followed by 2% human complement for 1 hour (S.E., n = 4). (D) ADCC in AQP4-expressing CHO cells incubated with 100,000 NK cells and 0.25–10 μg/ml untreated or IdeS-treated NMO-IgG (S.E., n = 4).

a Leica DM 4000 B fluorescence microscope at 25× magnification (Leica Microsystems, Buffalo Grove, IL). AQP4, GFAP, and myelin basic protein immunonegative areas were defined by hand and quantified using ImageJ (NIH, Bethesda, MD). Data are presented as the percentage of immunonegative area (normalized to total area of hemibrain slice). Protocols were approved by the University of California, San Francisco Committee on Animal Research.

Results

IdeS Cleavage of NMO-IgG Prevents CDC and ADCC. Figure 1A diagrams the binding of NMO-IgG to membrane-associated AQP4. IdeS cleavage occurs at the lower hinge/heavy chain constant region 2 of the IgG-class antibody to produce an $F(ab')_2$ fragment and two Fc fragments. SDS-PAGE with Coomassie Blue staining shows loss of the antibody heavy chain and appearance of smaller fragments following IdeS cleavage of NMO-IgG (Fig. 1B). Figure 1C verifies the IgG-selective action of IdeS. Purified human IgG, IgM, IgE, and IgA were treated with a high concentration of IdeS (5 U of IdeS/1 μg of immunoglobulin). Whereas cleavage of IgG was essentially complete under these conditions, showing bands at the expected molecular sizes of heavy chain fragments (31 kDa) and light chains (25 kDa), no cleavage was seen for IgM, IgE, or IgA.

Because IdeS separates $F(ab')_2$ from Fc, it is anticipated that Fc-dependent effector functions of NMO-IgG should be abolished following IdeS cleavage. Figure 2A shows loss of CDC, as measured by an Alamar Blue cytotoxicity assay, in AQP4-expressing cells incubated with control or IdeS-treated NMO-IgG, together with human complement. IdeS treatment prevented CDC caused by different monoclonal NMO-IgGs (left panel) and NMO patient sera (right panel). Figure 2B shows the time- and IdeS concentration-dependence for reduction of CDC for two monoclonal NMO-IgGs. Figure 2C shows that IdeS is effective when NMO-IgG is already bound to AQP4. AQP4-expressing cells were preincubated for 30 minutes with NMO-IgG, then IdeS was added, followed 30 minutes later by complement. IdeS treatment after NMO-IgG binding abolished CDC in a concentration-dependent manner. Figure 2D shows that IdeS cleavage abolished the ADCC effector function of NMO-IgG, as demonstrated in a cytotoxicity assay of AQP4-expressing cells incubated with NMO-IgG and human NK cells.

IdeS-Cleaved NMO-IgG Binds to AQP4, Competitively Displacing Pathogenic NMO-IgG. Binding of NMO-IgG to AQP4 was compared with that of the NMO-$F(ab')_2$ fragment generated by IdeS cleavage. Binding to AQP4-expressing cells was measured by a ratio imaging assay in which NMO-IgG was stained red [Cy3-conjugated $F(ab')_2$ fragment-specific antihuman secondary antibody] and AQP4 stained green (anti–C-terminal rabbit primary antibody, Alexa Fluor-488-antirabbit secondary antibody). Fluorescence micrographs show similar red fluorescence for control and IdeS-treated NMO-IgG, both for a recombinant NMO-IgG (Fig. 3A, left) and for NMO patient sera (Fig. 3B, left).

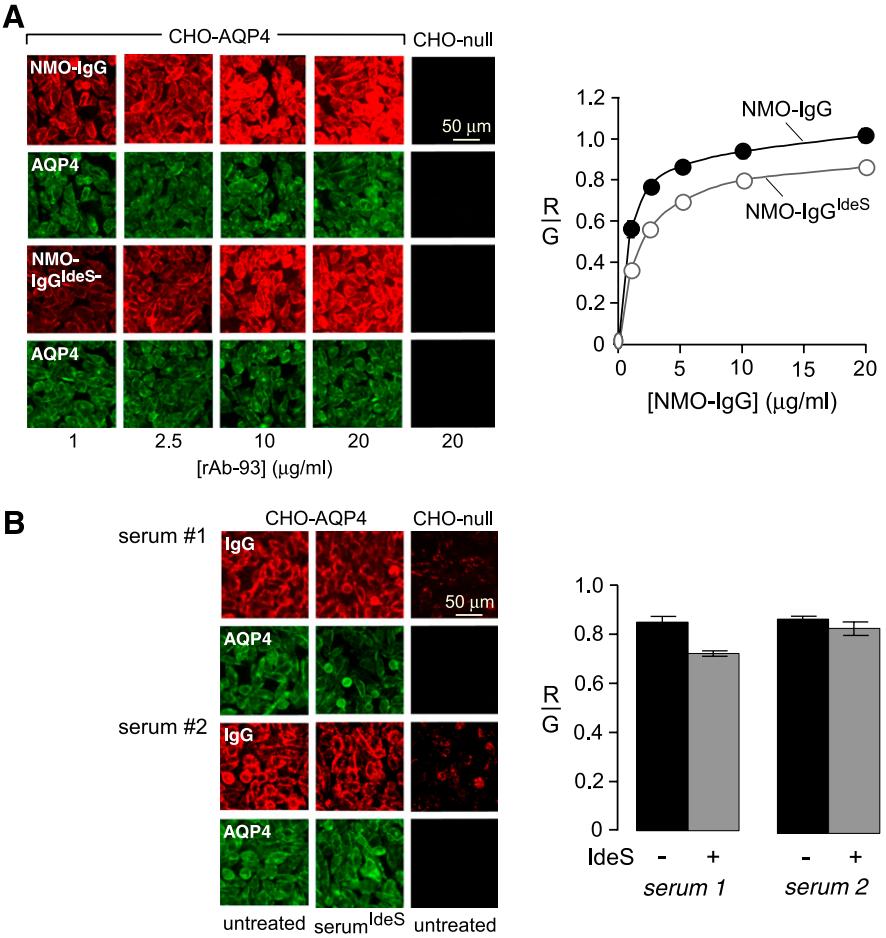

Fig. 3. IdeS-treated NMO-IgG binds to AQP4. (A) Binding of recombinant NMO-IgG (rAb-93) to AQP4 in AQP4-expressing CHO cells. (Left) Fluorescence micrographs showing $F(ab')_2$ binding (red) to AQP4 (green). (Right) Binding of NMO-IgG and NMO-IgG^{IdeS} showing red-to-green fluorescence ratio (R/G) as a function of NMO-IgG concentration (S.E., n = 3). (B) Binding of NMO patient sera to AQP4 in AQP4-expressing CHO cells. (Left) Fluorescence micrographs showing $F(ab')_2$ binding (red) to AQP4 (green). (Right) R/G at IgG concentrations of 200 and 50 μg/ml for sera 1 and 2, respectively (S.E., n = 3).

Quantitative ratio image analysis showed little effect of IdeS cleavage on NMO-IgG binding (Fig. 3, A and B, right).

The product NMO-F(ab′)$_2$ fragments, which lack effector functions, compete with the original NMO-IgG for binding to AQP4. NMO-IgG binding was measured using a horseradish peroxidase–conjugated secondary antibody that recognizes the Fc fragment of the primary antibody (Fig. 4A). NMO-IgG binding was greatly reduced with increasing concentrations of

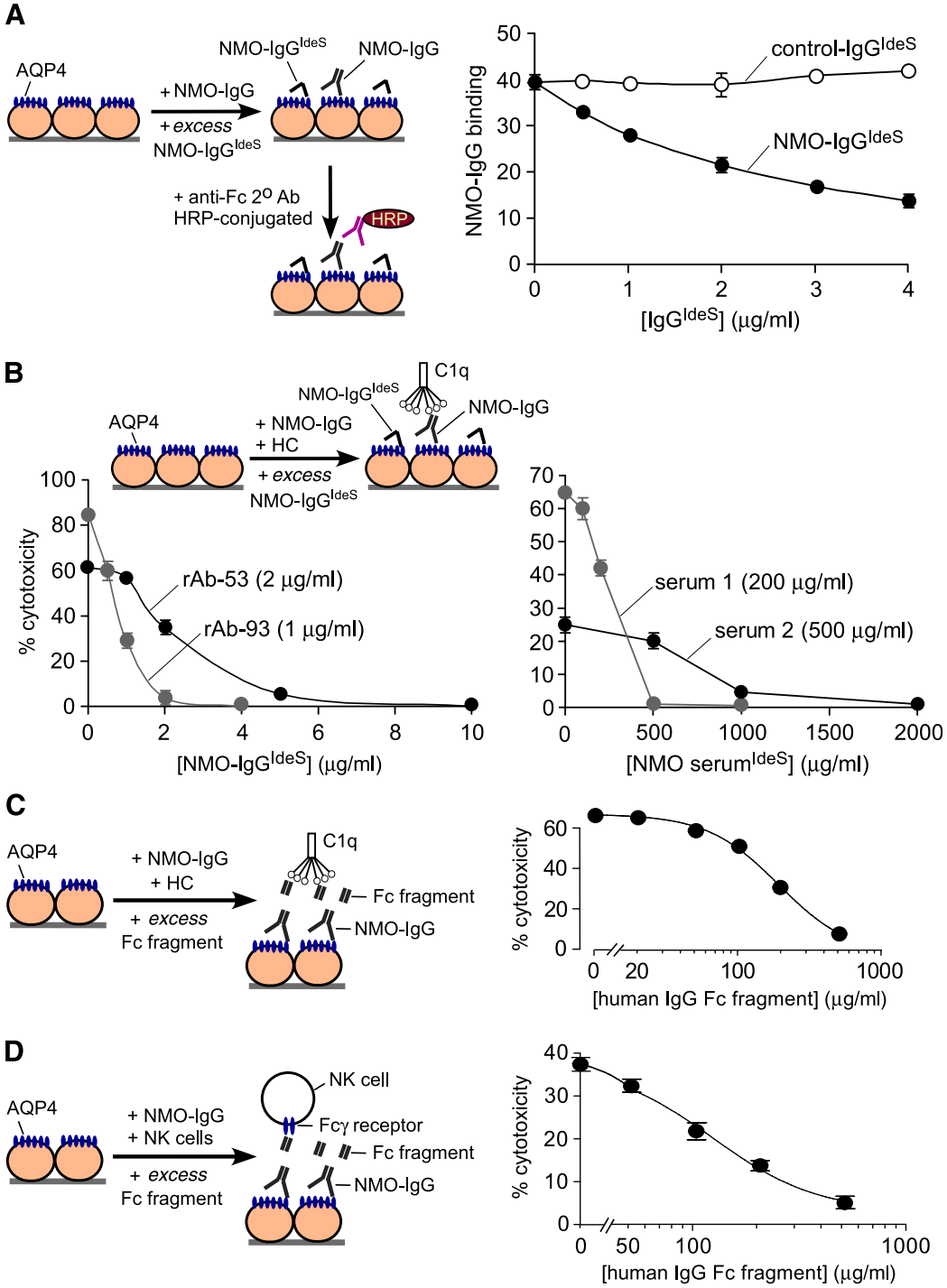

Fig. 4. IdeS-treated NMO-IgG competitively displaces pathogenic NMO-IgG, reducing cytotoxicity. (A) F(ab′)$_2$ fragments produced by IdeS cleavage of NMO-IgG competitively displaces NMO-IgG. Binding of NMO-IgG on AQP4-expressing CHO cells incubated with NMO-IgG (1 μg/ml rAb-93) and NMO-IgG^{IdeS} or control-IgG^{IdeS}, followed by horseradish peroxidase (HRP)-conjugated antihuman IgG (Fc-specific) secondary antibody, as quantified by an HRP activity assay. (B) IdeS-treated NMO-IgG protects against CDC caused by (untreated) NMO-IgG. Cytotoxicity measured by Alamar Blue assay after 60-minute incubation with NMO-IgG (2 μg/ml rAb-53; 1 μg/ml rAb-93) or NMO sera and 2% human complement (HC) in AQP4-expressing cells, together with indicated concentrations of NMO-IgG^{IdeS} or NMO serum^{IdeS} (S.E., n = 4). (C) Fc fragments generated by IdeS cleavage reduce CDC. AQP4-expressing CHO cells were incubated for 60 minutes with NMO-IgG (3 μg/ml rAb-53) and 1% human complement with different concentrations of human IgG Fc fragments. (D) Fc fragments reduce ADCC. Human IgG Fc fragments were preincubated with NK cells for 30 minutes at 37°C and then added together with NMO-IgG (3 μg/ml rAb-53) to AQP4-expressing CHO cells and incubated for 1 hour (S.E., n = 4).

IdeS-treated NMO-IgG (NMO-IgG^{IdeS}), but not of IdeS-treated control antibody (control-IgG^{IdeS}). In addition, CDC was measured in AQP4-expressing cells treated with different monoclonal NMO-IgGs or NMO patient sera together with complement, and increasing concentrations of IdeS-treated NMO-IgG. Figure 4B shows greatly reduced CDC with increasing concentrations of IdeS-treated NMO-IgG. IdeS cleavage thus converts pathogenic NMO-IgG into nonpathogenic, blocking NMO-F(ab′)$_2$ fragments that interfere with binding of pathogenic NMO-IgG to AQP4 and downstream cytotoxicity.

Fc Fragments Released after IdeS Cleavage Reduce CDC and ADCC. To test whether the IgG Fc fragments generated by IdeS can protect against NMO-IgG–induced CDC, AQP4-expressing cells were incubated with NMO-IgG, human complement, and different concentrations of human IgG Fc fragments. CDC was greatly reduced with inclusion of IgG Fc fragments (Fig. 4C). To test whether the IgG Fc fragments protect against NMO-IgG–induced ADCC, increasing concentrations of human IgG Fc fragments were added, together with NMO-IgG and human NK cells, to AQP4-expressing cells. Figure 4D shows that IgG Fc fragments prevented NMO-IgG–induced ADCC. The reduced CDC and ADCC are probably related to Fc fragment binding to C1q and Fcγ receptors, respectively.

IdeS Treatment Reduces NMO Pathology in Mice. IdeS was also tested in a mouse model of NMO produced by intracerebral injection of NMO-IgG and human complement (Saadoun et al., 2010, 2012). In a first set of studies, mice were injected with NMO-IgG (rAb-53), without or with IdeS pretreatment, together with complement. After three days there was marked loss of AQP4, GFAP, and myelin around the injection site in mice administered untreated NMO-IgG (Fig. 5A, left), as found previously (Saadoun et al., 2010), with only small lesions in mice receiving IdeS-treated NMO-IgG. Higher magnification of the lesion in mice receiving untreated NMO-IgG shows well demarcated areas of AQP4, GFAP, and myelin loss in the ipsilateral hemisphere, with increased expression of GFAP and AQP4 in reactive astrocytes outside of the lesion (Fig. 5A, center). Loss of GFAP, AQP4, and

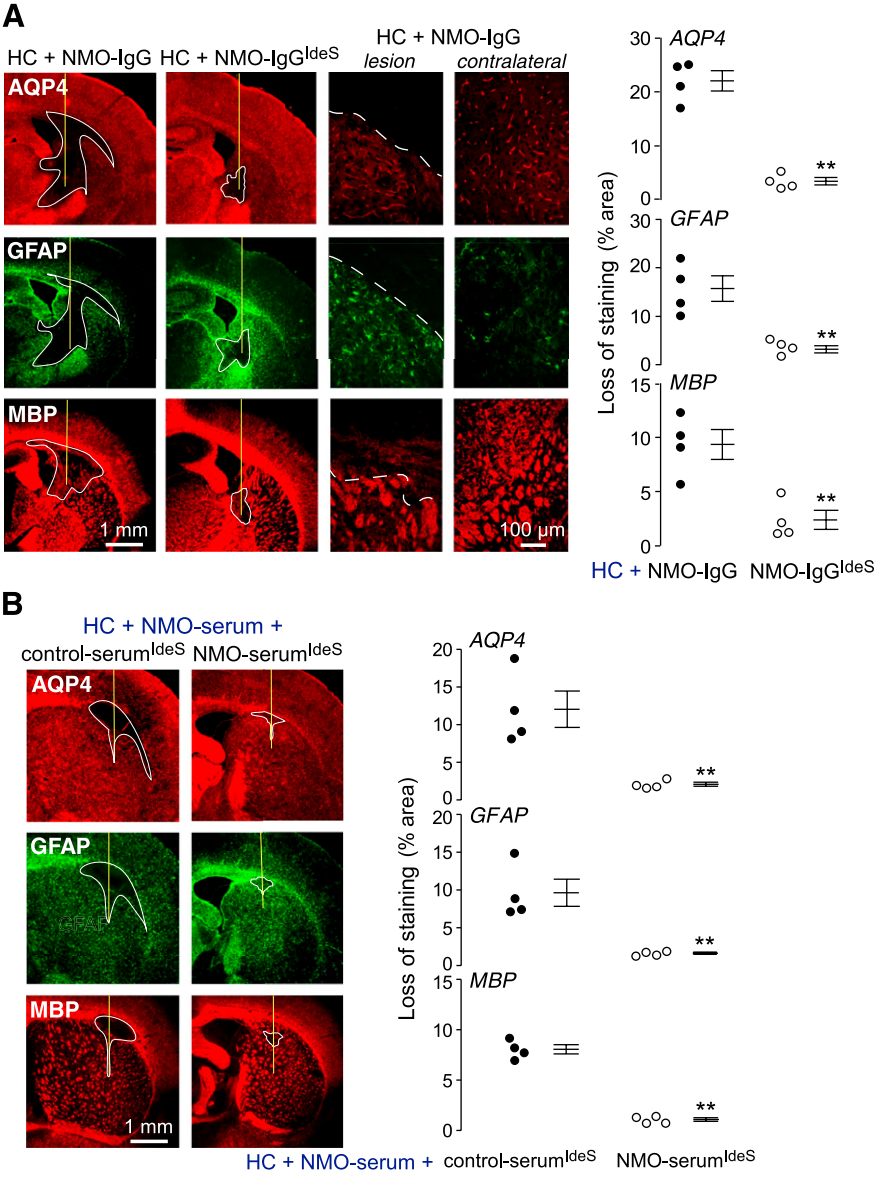

Fig. 5. IdeS treatment of NMO-IgG prevents lesions in a mouse model of NMO. (A) (left) Brains of live mice were injected with 0.6 μg NMO-IgG or NMO-IgG^{IdeS} together with 3 μl human complement (HC). Representative GFAP, AQP4, and myelin basic protein (MBP) immunofluorescence at three days after injection. The yellow line represents needle tract. The white line delimits the lesion with loss of AQP4, GFAP, and myelin. (center) Higher magnification of brains injected with NMO-IgG and HC. The white dashed line delimits the lesion (top). Contralateral hemispheres (noninjected) are shown (right). (Right) Summary of lesion size from experiments as in (A) (S.E., 4 mice per group; $^{**}P < 0.01$ by nonparametric Mann-Whitney test). (B) Brains were injected with 12 μg of purified IgG from NMO serum and 48 μg of IdeS-treated IgG purified from the same NMO patient (NMO serum^{IdeS}) or a non-NMO control (control serum^{IdeS}), together with 3 μl HC. (Left) Representative GFAP, AQP4, and MBP immunofluorescence at three days after injection. The yellow line shows the needle tract and the white line delimits the lesion. (Right) Summary lesion size (S.E., 4 mice per group; $^{**}P < 0.01$).

myelin immunoreactivity was greatly reduced in the mice receiving IdeS-treated NMO-IgG (Fig. 5A, right).

In a second set of experiments, mice were injected with untreated NMO-IgG (purified IgG from NMO patient serum) together with complement, without or with a 4-fold molar excess of IdeS-treated IgG from the same NMO patient. Figure 5B (left) shows typical lesions in mice receiving untreated NMO-IgG and complement, with much reduced lesion size when excess IdeS-treated NMO-IgG was included. Areas of loss of immunoreactivity are summarized in Fig. 5B (right). IdeS-treated NMO antibody can thus compete with pathogenic NMO antibody in mouse brain in vivo.

In a third set of in vivo experiments, mice were administered NMO-IgG (rAb-53) followed 15 minutes later by IdeS and complement at the same site. Figure 6A shows greatly reduced lesion size when IdeS was injected, with a summary of data in Fig. 6B. IdeS can thus cleave NMO-IgG already bound to astrocyte AQP4 in mouse brain in vivo at a sufficiently rapid rate to prevent the development of NMO lesions during exposure to complement.

Discussion

Therapeutic cleavage of NMO-IgG by the IgG-selective proteinase IdeS adds to the list of new candidate therapies that target pathogenic NMO autoantibodies. In general, therapeutic approaches for autoimmune diseases caused by pathogenic autoantibodies include 1) antibody removal by plasma exchange, 2) prevention of autoantibody binding to its target, and 3) antibody inactivation. Class 2 therapeutics include aquaporumab-blocking antibodies (Tradtrantip et al., 2012b) and small-molecule blockers (Tradtrantip et al., 2012a) that compete sterically with pathogenic NMO autoantibodies for binding to AQP4. The blocking strategy involves the engineering or identification of a nonpathogenic-blocking molecule with sufficiently high AQP4 binding affinity and concentration at the target site to competitively displace polyclonal, pathogenic autoantibodies in NMO serum. The antibody inactivation strategy is conceptually simple and potentially more practical compared with blocker strategies. The ideal antibody inactivation strategy would produce selective inactivation of NMO-IgG, although nonselective IgG inactivation has the potential benefit of inactivating alternative IgGs that might contribute to NMO pathology such as antibodies against myelin-oligodendrocyte glycoprotein (Kitley et al., 2012). Because human NMO-IgG autoantibodies are of the IgG1 class, selective IgG1 inactivation would also be an attractive approach; however, the most selective available endoglycosidases and proteinases inactivate all IgG subclasses (Collin and Olsén, 2001a; von Pawel-Rammingen et al., 2002). We found here that IdeS neutralized NMO-IgG pathogenicity, abolishing CDC and ADCC effector functions, and yielding therapeutic $F(ab')_2$ and Fc fragments that blocked NMO-IgG binding to AQP4 and Fcγ receptors, respectively. IdeS efficiently cleaved both free and AQP4-bound NMO-IgG, without effect on AQP4 binding of the product NMO-$F(ab')_2$ fragment.

Data from animal models support the therapeutic utility of IdeS for autoimmune diseases caused by pathogenic autoantibodies. In mice, IdeS treatment has been shown to prevent collagen antibody-induced arthritis (Nandakumar et al., 2007), antiplatelet IgG-induced thrombocytopenia (Johansson et al., 2008), and antiglomerular basement membrane-induced glomerulonephritis (Yang et al., 2010). The cleavage of IgG

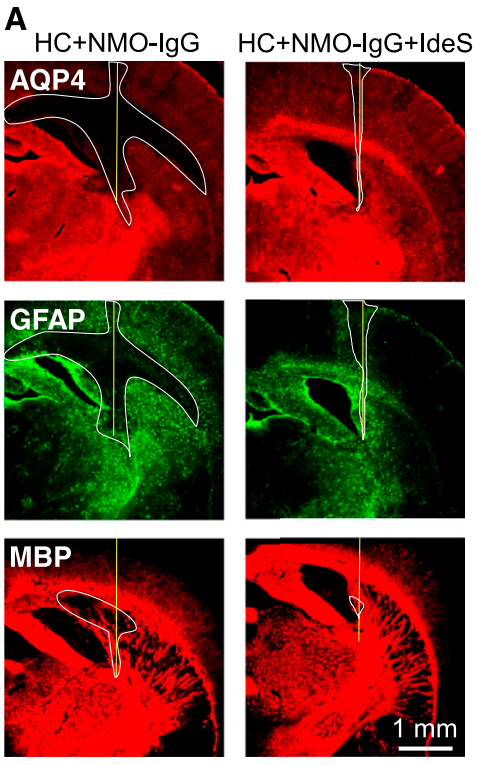

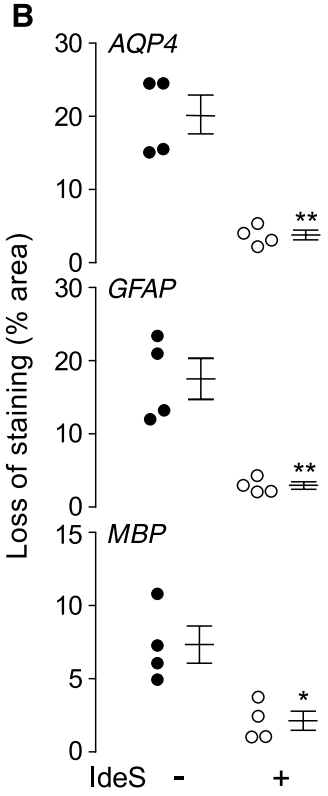

Fig. 6. EndoS efficiently cleaves NMO-IgG in mice in vivo. Injected IdeS reduces NMO lesions in mouse brain. Mice were injected with 0.6 μg of NMO-IgG and, 15 minutes later at the same site, 3 μl of human complement (HC) without or with 16.75 U of IdeS. (A) Representative GFAP, AQP4, and myelin basic protein (MBP) immunofluorescence at three days after injection. The yellow line represents needle tract. The white line delimits the lesion with loss of AQP4, GFAP, and myelin. (B) Summary of lesion size from experiments as in (A) (S.E., 4 mice per group; $^*P < 0.05$; $^{**}P < 0.01$ by nonparametric Mann-Whitney test).

following intravenous administration of IdeS in mice and rabbits is rapid and efficient, and well tolerated even at high IdeS concentrations (Nandakumar et al., 2007; Johansson et al., 2008). As reported (von Pawel-Rammingen et al., 2002) and verified here, IdeS has high selectivity for IgG; other cysteine proteases such as streptopain have broad proteolytic activity (Collin and Olsén, 2001b). Notwithstanding the successful use of IdeS when administered to animals, repeated intravenous administration of IdeS in humans would likely elicit an immune response. However, even though most humans who have been infected with *S. pyogenes* have antibodies against streptococcal proteins including IdeS (Akesson et al., 2004), these neutralizing antibodies do not interfere with the IgG-cleaving action of IdeS (Johansson et al., 2008). An immune response against IdeS is unlikely to occur if patient serum is exposed to membrane-immobilized IdeS by extracorporeal circulation in therapeutic apheresis.

We found efficient cleavage of AQP4-bound NMO-IgG when administered by intracerebral injection. IdeS cleavage of NMO-IgG was sufficiently rapid to prevent NMO lesions in mouse brain after NMO-IgG was already bound to AQP4, in which IdeS and complement were coadministered 15 minutes after NMO-IgG. A similar experiment with EndoS (coadministration of EndoS + complement after NMO-IgG) was not successful (unpublished data), probably because of the lower enzymatic activity of EndoS compared with IdeS. The greater efficacy of IdeS compared with EndoS was also demonstrated in a mouse model of experimental glomerulonephritis (Yang et al., 2010).

In conclusion, IdeS cleavage represents a compelling therapeutic strategy for NMO autoantibody neutralization, as it efficiently and completely abolishes NMO-IgG effector functions, and produces therapeutic $F(ab')_2$ and Fc fragments. IdeS cleavage may be accomplished by therapeutic apheresis in which patient blood is passed over surface-immobilized IdeS. Alternatively, notwithstanding potential concerns about immunogenicity, IdeS might be administered by intravenous injection, or by intrathecal or retro-orbital routes to target NMO lesions with minimal systemic exposure.

Acknowledgments

The authors thank Dr. Jeffrey L. Bennett (University of Colorado, Denver) for providing recombinant monoclonal AQP4-IgGs.

Authorship Contributions

Participated in research design: Tradtrantip, Asavapanumas, Verkman.

Conducted experiments: Tradtrantip, Asavapanumas.

Performed data analysis: Tradtrantip, Asavapanumas.

Wrote or contributed to the writing of the manuscript: Tradtrantip, Asavapanumas, Verkman.

References

Akesson P, Rasmussen M, Mascini E, von Pawel-Rammingen U, Janulczyk R, Collin M, Olsen A, Mattsson E, Olsson ML, and Bjorck L et al. (2004) Low antibody levels against cell wall-attached proteins of Streptococcus pyogenes predispose for severe invasive disease. *J Infect Dis* **189**:797–804.

Bennett JL, Lam C, Kalluri SR, Saikali P, Bautista K, Dupree C, Glogowska M, Case D, Antel JP, and Owens GP et al. (2009) Intrathecal pathogenic anti-aquaporin-4 antibodies in early neuromyelitis optica. *Ann Neurol* **66**:617–629.

Collin M and Olsén A (2001a) EndoS, a novel secreted protein from *Streptococcus pyogenes* with endoglycosidase activity on human IgG. *EMBO J* **20**:3046–3055.

Collin M and Olsén A (2001b) Effect of SpeB and EndoS from *Streptococcus pyogenes* on human immunoglobulins. *Infect Immun* **69**:7187–7189.

Collongues N and de Seze J (2011) Current and future treatment approaches for neuromyelitis optica. *Ther Adv Neurol Disord* **4**:111–121.

Crane JM, Lam C, Rossi A, Gupta T, Bennett JL, and Verkman AS (2011) Binding affinity and specificity of neuromyelitis optica autoantibodies to aquaporin-4 M1/M23 isoforms and orthogonal arrays. *J Biol Chem* **286**:16516–16524.

Cree B (2008) Neuromyelitis optica: diagnosis, pathogenesis, and treatment. *Curr Neurol Neurosci Rep* **8**:427–433.

Jarius S, Paul F, Franciotta D, Waters P, Zipp F, Hohlfeld R, Vincent A, and Wildemann B (2008) Mechanisms of disease: aquaporin-4 antibodies in neuromyelitis optica. *Nat Clin Pract Neurol* **4**:202–214.

Jarius S and Wildemann B (2010) AQP4 antibodies in neuromyelitis optica: diagnostic and pathogenetic relevance. *Nat Rev Neurol* **6**:383–392.

Johansson BP, Shannon O, and Bjorck L (2008) IdeS: a bacterial proteolytic enzyme with therapeutic potential. *PLoS one* **3**:e1692.

Kim SH, Kim W, Huh SY, Lee KY, Jung IJ, and Kim HJ (2013) Clinical efficacy of plasmapheresis in patients with neuromyelitis optica spectrum disorder and effects on circulating anti-aquaporin-4 antibody levels. *J Clin Neurol* **9**:36–42.

Kira J (2011) Autoimmunity in neuromyelitis optica and opticospinal multiple sclerosis: astrocytopathy as a common denominator in demyelinating disorders. *J Neurol Sci* **311**:69–77.

Kitley J, Woodhall M, Waters P, Leite MI, Devenney E, Craig J, Palace J, and Vincent A (2012) Myelin-oligodendrocyte glycoprotein antibodies in adults with a neuromyelitis optica phenotype. *Neurology* **79**:1273–1277.

Lennon VA, Kryzer TJ, Pittock SJ, Verkman AS, and Hinson SR (2005) IgG marker of optic-spinal multiple sclerosis binds to the aquaporin-4 water channel. *J Exp Med* **202**:473–477.

Lucchinetti CF, Mandler RN, McGavern D, Bruck W, Gleich G, Ransohoff RM, Trebst C, Weinshenker B, Wingerchuk D, and Parisi JE et al. (2002) A role for humoral mechanisms in the pathogenesis of Devic's neuromyelitis optica. *Brain* **125**:1450–1461.

Nandakumar KS, Johansson BP, Bjorch L, and Holmdahl R (2007) Blocking of experimental arthritis by cleavage of IgG antibodies in vivo. *Arthritis Rheum* **56**:3235–3260.

Nielsen S, Nagelhus EA, Amiry-Moghaddam M, Bourque C, Agre P, and Ottersen OP (1997) Specialized membrane domains for water transport in glial cells: high-resolution immunogold cytochemistry of aquaporin-4 in rat brain. *J Neurosci* **17**:171–180.

Papadopoulos MC and Verkman AS (2012) Aquaporin 4 and neuromyelitis optica. *Lancet Neurol* **11**:535–544.

Papadopoulos MC and Verkman AS (2013) Aquaporin water channels in the nervous system. *Nat Rev Neurosci* **14**:265–277.

Phuan PW, Ratelade J, Rossi A, Tradtrantip L, and Verkman AS (2012) Complement-dependent cytotoxicity in neuromyelitis optica requires aquaporin-4 protein assembly in orthogonal arrays. *J Biol Chem* **287**:13829–13839.

Saadoun S, Waters P, Bell BA, Vincent A, Verkman AS, and Papadopoulos MC (2010) Intra-cerebral injection of neuromyelitis optica immunoglobulin G and human complement produces neuromyelitis optica lesions in mice. *Brain* **133**:349–361.

Saadoun S, Waters P, MacDonald C, Bell BA, Vincent A, Verkman AS, and Papadopoulos MC (2012) Neutrophil protease inhibition reduces neuromyelitis optica-immunoglobulin G-induced damage in mouse brain. *Ann Neurol* **71**:323–333.

Sato D, Callegaro D, Lana-Peixoto MA, and Fujihara K; Brazilian Committee for Treatment and Research in Multiple Sclerosis (2012) Treatment of neuromyelitis optica: an evidence based review. *Arq Neuropsiquiatr* **70**:59–66.

Tradtrantip L, Ratelade J, Zhang H, and Verkman AS (2013) Enzymatic deglycosylation converts pathogenic neuromyelitis optica anti-aquaporin-4 immunoglobulin G into therapeutic antibody. *Ann Neurol* **73**:77–85.

Tradtrantip L, Zhang H, Anderson MO, Saadoun S, Phuan PW, Papadopoulos MC, Bennett JL, and Verkman AS (2012a) Small-molecule inhibitors of NMO-IgG binding to aquaporin-4 reduce astrocyte cytotoxicity in neuromyelitis optica. *FASEB J* **26**:2197–2208.

Tradtrantip L, Zhang H, Saadoun S, Phuan PW, Lam C, Papadopoulos MC, Bennett JL, and Verkman AS (2012b) Anti-aquaporin-4 monoclonal antibody blocker therapy for neuromyelitis optica. *Ann Neurol* **71**:314–322.

Vincents B, von Pawel-Rammingen U, Björck L, and Abrahamson M (2004) Enzymatic characterization of the streptococcal endopeptidase, IdeS, reveals that it is a cysteine protease with strict specificity for IgG cleavage due to exosite binding. *Biochemistry* **43**:15540–15549.

von Pawel-Rammingen U, Johansson BP, and Björck L (2002) IdeS, a novel streptococcal cysteine proteinase with unique specificity for immunoglobulin G. *EMBO J* **21**:1607–1615.

Wingerchuk DM, Lennon VA, Lucchinetti CF, Pittock SJ, and Weinshenker BG (2007) The spectrum of neuromyelitis optica. *Lancet Neurol* **6**:805–815.

Wingerchuk DM, Lennon VA, Pittock SJ, Lucchinetti CF, and Weinshenker BG (2006) Revised diagnostic criteria for neuromyelitis optica. *Neurology* **66**:1485–1489.

Yang R, Otten MA, Hellmark T, Collin M, Björck L, Zhao MH, Daha MR, and Segelmark M (2010) Successful treatment of experimental glomerulonephritis with IdeS and EndoS, IgG-degrading streptococcal enzymes. *Nephrol Dial Transplant* **25**:2479–2486.

Address correspondence to: Dr. Alan S. Verkman, 1246 Health Sciences East Tower, Box 0521, University of California, San Francisco, CA 94143-0521. E-mail: Alan.Verkman@ucsf.edu